RESEARCH PAPER

Channels 3:4, 277-286; July/August 2009; © 2009 Landes Bioscience

Gating currents from neuronal $K_V7.4$ channels
General features and correlation with the ionic conductance

Francesco Miceli,[1-3] Maria Roberta Cilio,[2] Maurizio Taglialatela[1,4,*] and Francisco Bezanilla[3,*]

[1]Section of Pharmacology; Department of Neuroscience; University of Naples Federico II; Naples, Italy; [2]Division of Neurology; IRCCS Bambino Gesù Children's Hospital; Rome, Italy; [3]Department of Biochemistry and Molecular Biology; The University of Chicago; Chicago, IL USA; [4]Department of Health Science; University of Molise; Campobasso, Italy

Key words: potassium channels, gating currents, K_V7, epilepsy, deafness, voltage-sensing domain

Abbreviations: K^+, potassium; VGKCs, voltage-gated potassium channels; VSD, voltage-sensing domain; I_{KM}, M-current; DFNA2, slowly progressive deafness with autosomal-dominant hereditary transmission; BFNS, benign familial neonatal seizures; COVC, cut-open voltage-clamp technique; NMG, N-Methy-D-Glucamine; MES acid, methane sulfonic acid; TEA, tetraethylammonium; *G/V*, conductance-voltage; G, conductance; Q, gating charge; τ, time constant; Q_{ON},ON gating charge; Q_{OFF}, OFF gating charge; I(V), macroscopic current; n, number of channels; i(V), single-channel current; P_o(V), opening probability

The K_V7 (KCNQ) subfamily of voltage-gated K^+ channels consists of five members ($K_V7.1$-$K_V7.5$) giving rise to non-inactivating, and slowly activating/deactivating currents mainly expressed in cardiac ($K_V7.1$) and neuronal ($K_V7.2$-$K_V7.5$) tissue. In the present study, using the cut-open oocyte voltage clamp, we studied the relation of the ionic currents from homomeric neuronal K_V7 channels ($K_V7.2$-$K_V7.5$) with the gating currents recorded after K^+ conductance blockade from the same channels. Increasing the recording temperature from 18°C to 28°C accelerated activation/deactivation kinetics of the ionic currents in all homomeric K_V7 channels (activation Q_{10}s at 0 mV were 3.8, 4.1, 8.3 and 2.8 for $K_V7.2$, $K_V7.3$, $K_V7.4$ and $K_V7.5$ channels, respectively), without large changes in currents voltage-dependence; moreover, at 28°C, ionic currents carried by $K_V7.4$ channels also showed a significant increase in their maximal value. Gating currents were only resolved in $K_V7.4$ and $K_V7.5$ channels; the size of the ON gating charges at +40 mV was 1.34 ± 0.34 nC for $K_V7.4$, and 0.79 ± 0.20 nC for $K_V7.5$. At 28°C, $K_V7.4$ gating currents had the following salient properties: (1) similar time integral of Q_{ON} and Q_{OFF}, indicating no charge immobilization; (2) a left-shift in the $V_{1/2}$ of the Q_{ON}/V when compared to the G/V (≈50 mV in the presence of 2 mM extracellular Ba^{2+}); (3) a Q_{ON} decay faster than ionic current activation; and (4) a rising phase in the OFF gating charge after depolarizations larger than 0 mV. These observations suggest that, in $K_V7.4$ channels, VSD movement is followed by a slow and/or low bearing charge step linking to pore opening, a result which may help to clarify the molecular consequence of disease-causing mutations and drugs affecting channel gating.

Introduction

Voltage-gated potassium (K^+) channels (VGKCs) are membrane proteins, which undergo conformational changes that lead to the opening of the K^+-selective pore in response to changes in membrane potentials. In neuronal cells, VDKCs play a critical role in setting the resting membrane potential, in action potential repolarization, and in controlling firing frequency and neurotransmitter release. VGKCs also regulate skeletal and smooth muscle contraction, cell volume, proliferation and differentiation, as well as hormonal secretion. Structurally, VGKCs are homomeric or heteromeric membrane proteins formed upon assembly of four identical or compatible subunits, respectively. Each subunit is composed of six transmembrane segments (S_1-S_6); the S_5 and S_6 segments and the intervening linker provide a major contribution to the formation of the K^+-selective aqueous pore and the inner pore gate, whereas the S_1-S_4 region forms the voltage sensor domain (VSD).[1]

The molecular and functional diversity of the VGKC family is astonishing, with each member characterized by distinct biophysical, pharmacological and regulatory properties.[1] In particular, the K_V7 (KCNQ) subfamily consists of five members ($K_V7.1$-$K_V7.5$), each showing a specific tissue distribution and pathophysiological role.[2] In fact, $K_V7.1$ is mainly expressed in the heart, whereas $K_V7.2$-5 subunits have a prevalent neuronal location; this canonical view has been recently challenged by the discovery that some "neuronal" K_V7 subunits, are also expressed in skeletal[3,4] and smooth[5] muscle cells. While $K_V7.1$ subunits underlie the slow component of the cardiac repolarizing current I_{Ks} which contributes to the late phase of action potential repolarization,[6-8] $K_V7.2$,

*Correspondence to: Maurizio Taglialatela; Email: m.taglialatela@unimol.it / Francisco Bezanilla; Email: fbezanilla@uchicago.edu
Submitted: 05/22/09; Revised: 07/08/09; Accepted: 07/09/09
Previously published online: www.landesbioscience.com/journals/channels/article/9477

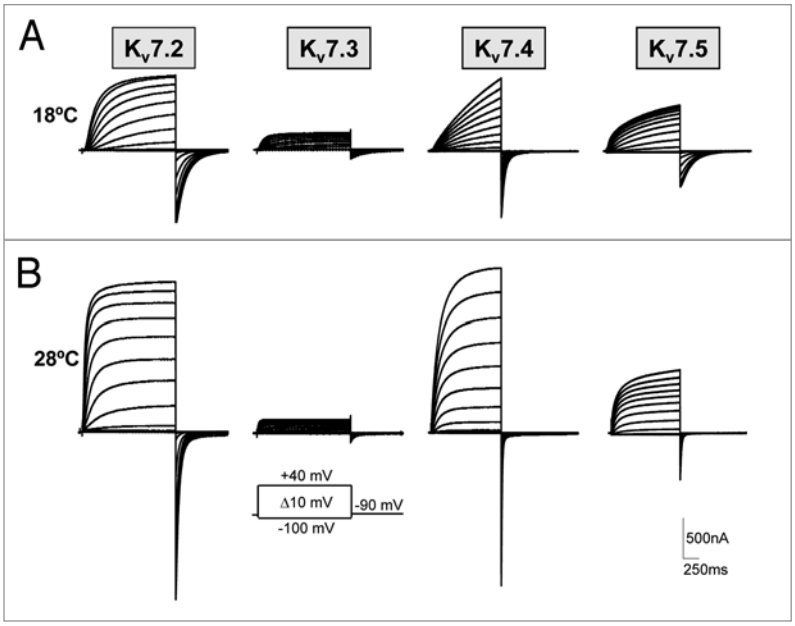

Figure 1. Ionic currents from neuronal K_V7 channels expressed in *Xenopus* oocytes recorded at 18°C (A) and at 28°C (B). Currents were elicited in response to test pulses from -100 to +40 mV in 10 mV increments from and returning to an holding potential of -90 mV.

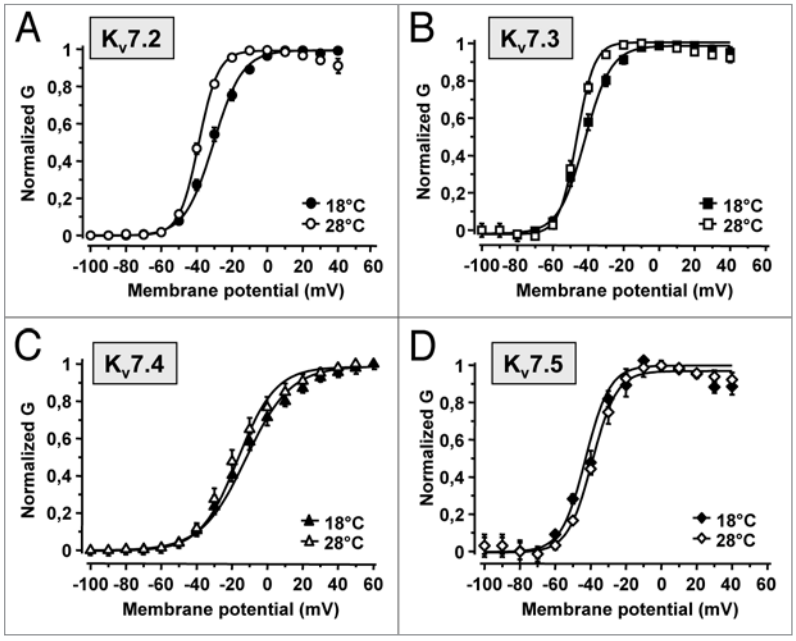

Figure 2. Effect of temperature on the steady-state activation properties of the macroscopic currents carried by neuronal K_V7 channels. G/V curves from $K_V7.2$ (A), $K_V7.3$ (B), $K_V7.4$ (C) and $K_V7.5$ (D) channels. Continuous lines represent Boltzmann fits of the experimental data. In all panels, filled and empty symbols refer to data recorded at 18°C and 28°C, respectively. Each data point is the Mean ± SEM of 4–9 determinations for each group.

$K_V7.3$, $K_V7.4$ and $K_V7.5$ subunits, either as homomultimers or heteromultimers, represent the molecular basis of the M-current (I_{KM}), a K^+-selective, non-inactivating, and slowly activating/deactivating neuronal current.[9] I_{KM} has profound effects on neuronal excitability, contributing to the K^+ conductance at threshold membrane potential values for spike initiation and acting as a brake for repetitive firing. $K_V7.4$ subunits are also expressed in cochlear and vestibular organs of the inner hear, as well as in central auditory pathways.[10]

Loss of function mutations in four of the five K_V7 genes lead to distinct inherited diseases. $K_V7.1$ mutations are responsible for dominant (the Romano-Ward syndrome) and recessive (the Jervell and Lange-Nielsen syndrome) chromosome 11-linked forms of the long QT syndrome.[8] Mutations in $K_V7.4$ underlie a slowly progressive deafness with autosomal-dominant hereditary transmission (DFNA2),[10] whereas gene defects affecting $K_V7.2$ and, more rarely, $K_V7.3$ genes have been identified in families affected by Benign Familial Neonatal Seizures (BFNS), an autosomal-dominant inherited epilepsy of the newborn.[11-13] In all these diseases, several missense mutations have been described affecting residues located within the VSD, and changes in gating properties of the macroscopic currents are believed to represent a crucial pathogenetic mechanism to explain the decreased activity of the affected channels.[11-18] Moreover, drugs interfering with neuronal K_V7 channels gating represent novel therapeutic tools against hyperexcitability diseases in humans.[2]

Gating currents are transient currents generated by the displacement of charged elements within the VSD in response to changes in transmembrane voltage; therefore, gating current recordings provide crucial insights into the channel structural rearrangements during the gating process. Although gating currents were originally described for ion channels in their native environment,[19] heterologous expression systems allow to dissect the molecular basis for these structural transitions and to reveal essential elements of the channel protein contributing to gating currents.[20,21] Gating currents are roughly two orders of magnitude smaller than the ionic currents; therefore, gating currents resolution requires a sufficiently high density of channels in the membrane, together with a complete block of their ion permeation.[22,23] For VGKCs, gating current recordings in $K_V1.1$,[24] $K_V2.1$,[25] $K_V1.5$,[26] $K_{Ca}1.1$,[27] $K_V4.2$,[28] $K_V10.1$,[29] and $K_V11.1$,[30] have allowed to describe the molecular basis for peculiar kinetic or steady-state ionic current behavior, to gain a deeper understanding of the structure-function relationships for these channels, and in some cases, to unveil the pathophysiological role of specific residues affected in genetic channelopathies.

In the present, study we have addressed some of these challenging issues in neuronal K_V7 channels, a highly pathophysiologically relevant family of VGKCs whose macroscopic current gating behavior is characterized by extremely slow activation and deactivation kinetics. Using the cut-open

Table 1. Steady-state activation and size of the macroscopic currents carried by neuronal K_V7 channels expressed in *Xenopus* oocytes and recorded at 18°C and 28°C

		18°C			28°C		
	n	$V_{1/2}$ (mV)	k (e/fold)	I at +40 mV (pA)	$V_{1/2}$ (mV)	k (e/fold)	I at +40 mV (pA)
$K_V7.2$	9	-30.4 ± 0.8	8.2 ± 0.5	968.20 ± 208.32	-38.7 ± 0.8*	5.5 ± 0.4*	1571.58 ± 309.47
$K_V7.3$	5	-41.9 ± 0.9	7.4 ± 0.6	153.62 ± 40.16	-46.5 ± 1.3	4.9 ± 0.7*	175.41 ± 42.71
$K_V7.4$	4	-12.1 ± 1.4	12.7 ± 0.7	677.83 ± 181	-16.7 ± 1.4	10.7 ± 0.6	1736.45 ± 221.05*
$K_V7.5$	6	-42.9 ± 2.4	6.9 ± 1.7	547.40 ± 56.84	-39.2 ± 0.6	6.9 ± 0.7	849.94 ± 277.48

*values significantly different ($p < 0.05$) from those recorded at 18°C.

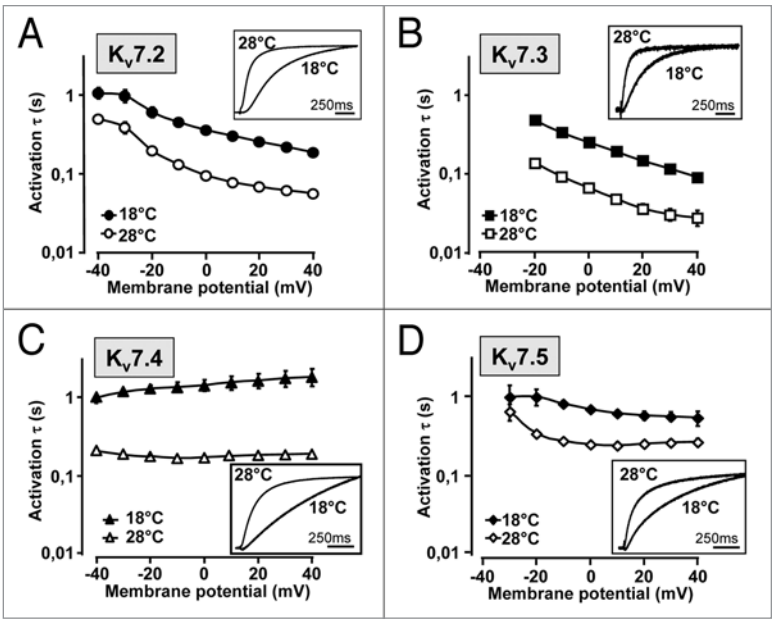

Figure 3. Effect of temperature on the activation kinetics of the macroscopic currents carried by neuronal K_V7 channels. Activation time constants of $K_V7.2$ (A), $K_V7.3$ (B), $K_V7.4$ (C) and $K_V7.5$ (D) homomeric channels. In all panels, filled and empty symbols refer to data recorded at 18°C and 28°C, respectively; the inserts show representative current traces recorded at 0 mV from each channel at 18°C and 28°C, as indicated.

vaseline gap voltage-clamp technique in *Xenopus* oocytes expressing neuronal K_V7 channels, we provide the first evidence that gating currents can be faithfully recorded from $K_V7.4$ and $K_V7.5$ channels, and we describe here their general features.

Results

Effect of a 10°C increase in the recording temperature on $K_V7.2$-5 ionic currents. Homomeric channels formed by K_V7 subunits are characterized by their slow gating. Since the ability to record gating currents is critically dependent on the speed of the gating charge movement, in a first series of experiments we attempted to accelerate the gating process by increasing the recording temperature. In fact, temperature is known to have important effects on channel gating kinetics and on gating charge movements,[34] although the intrinsic temperature sensitivity of this process varies widely among different channels.[34,35] In particular, the effect of temperature on steady-state voltage-dependence and kinetics of activation, as well on the maximal current, were evaluated for homomeric channels formed by each neuronal K_V7 subunit expressed in *Xenopus* oocytes.

The upper panel of **Figure 1** shows macroscopic ionic currents from homomeric $K_V7.2$-5 channels recorded at 18°C. All four channel subtypes displayed voltage-dependent and K^+-selective currents characterized by a rather slow time course of activation and deactivation, and a threshold for current activation around -40 mV; the size of the macroscopic current was the smallest for channels encoded by the $K_V7.3$ gene. Furthermore, $K_V7.4$ channels displayed the slowest activation kinetics. A 10°C increase in the recording temperature (from 18°C to 28°C) altered the activation kinetics of all four channels, with $K_V7.4$ showing the largest effect (**Fig. 1**, lower). In order to quantify the voltage-dependence of activation for each channel, conductance (G) values were calculated as described in the Materials and Methods section, expressed as a function of the applied voltages, and fitted to a Boltzmann equation. **Figure 2** shows the normalized G/V curves for each channel subtype recorded at 18°C and 28°C; the resulting $V_{1/2}$ and k values are listed in **Table 1**. A 10°C increase in recording temperature failed to cause large changes in the steady-state voltage-dependence of the macroscopic currents in $K_V7.4$ and $K_V7.5$ channels. $K_V7.2$ channels showed a significant 8 mV hyperpolarizing shift in $V_{1/2}$, together with a decrease in the slope factor k. A decrease in the slope factor k was also observed in $K_V7.3$ channels, without significant changes in $V_{1/2}$. Moreover, increasing the recording temperature caused a significant ($p < 0.05$) increase in the size of the macroscopic current only for $K_V7.4$ channels (about 250%, although this number may be smaller because at low temperature the currents had not settled), with $K_V7.2$ and $K_V7.5$ channels showing a similar trend (about 50% increase), although these effect did not reach statistical significance ($p > 0.05$).

Kinetic analysis of the activation process revealed a dramatic decrease in the activation time constants (τ) by increasing temperatures for all neuronal K_V7 channels, with Q_{10} values of 3.8, 4.1, 8.3 and 2.8 for $K_V7.2$, $K_V7.3$, $K_V7.4$ and $K_V7.5$ channels, respectively (**Fig. 3**). Therefore, $K_V7.4$ channels, in addition to the previously reported increase in maximal current size, also

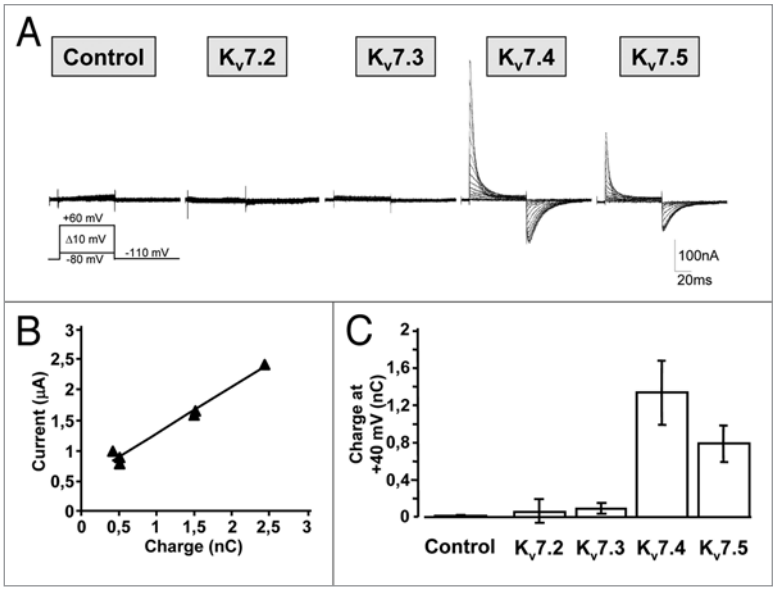

Figure 4. Currents recorded from *Xenopus* oocytes expressing neuronal K_V7 channels after blockade of the macroscopic K^+ conductance. (A) Representative current traces recorded at 28°C from the indicated neuronal K_V7 channels after blockade of the ionic current with TEA (both extracellular and intracellular) and 2 mM Ba^{2+} (extracellular). From an holding potential of -90 mV, after a short hyperpolarizing potential at -110 mV, currents were elicited in response to a series of depolarizations from -80 to +80 mV (in 10 mV increments), followed by a final step to -110 mV. (B) Direct correlation between the size of the instantaneous transient currents and the macroscopic ionic currents. Gating charge was calculated as described in the Materials and Methods section, after ionic current blockade. (C) Averaged values of Q_{ON} at +40 mV for the indicated experimental groups. Each bar is the Mean ± SEM of 4–9 cells for each group.

showed the highest temperature sensitivity in their activation kinetics.

Gating currents from $K_V7.4$ and $K_V7.5$ channels. *General features.* Because of the small expected size of the gating currents, one of the most challenging technical issues for gating current recordings is the need to completely suppress the ionic currents; for K^+ channels, this requires the addition of blockers and/or the absence of permanent ions, or the use of mutant channels unable to permeate but still able to give rise to gating currents.[36] Therefore, in the present experiments, intracellular and extracellular solutions in which K^+ ions were substituted with iso-osmolar concentrations of the pore blocker TEA were used; however, despite the well-known differences in TEA blocking affinity among various neuronal K_V7 subunits,[3,37] under these recording conditions, full blockade of the ionic currents was not achieved (data not shown). Therefore, we also exploited the strong I_{KM} sensitivity to blockade by extracellular Ba^{2+} ions of neuronal K_V7 channels,[10,38-40] and added 2 mM Ba^{2+} to the extracellular solution.

Figure 4A shows the current traces evoked by depolarizing pulses from -80 to +60 mV (10 mV steps) recorded in oocytes expressing $K_V7.2$, $K_V7.3$, $K_V7.4$ and $K_V7.5$ channels at 28°C using the previously described intracellular and extracellular solutions. While no active voltage-dependent currents could be detected from uninjected oocytes and from oocytes expressing $K_V7.2$ and $K_V7.3$ channels, fast and transient time- and voltage-dependent currents could be clearly seen from $K_V7.4$- and $K_V7.5$-expressing oocytes. These currents were outwardly directed upon depolarization, and inwardly directed upon return to hyperpolarized voltages. During depolarization, the outward currents showed a quasi-instantaneous activation, followed by a decay, which was faster during stronger depolarization; by contrast, the inward currents recorded upon repolarization showed a rising phase followed by a slower time-dependent decay. These characteristics, together with the observation that similar currents were not detected in uninjected oocytes or in oocytes expressing $K_V7.2$ or $K_V7.3$ channels, suggested that these currents were related to the expression of $K_V7.4$ or $K_V7.5$ channels in the oocyte membrane, and that they represented the gating currents from these channels; the transient outward and inward currents recorded under these conditions would arise from the ON (Q_{ON}) and OFF (Q_{OFF}) gating charge movement for these channels, respectively. For $K_V7.4$ channels, this conclusion appears also to be supported by the direct correlation between the size of the instantaneous transient currents recorded upon blockade of the ionic current and the size of the ionic current before channel blockade (**Fig. 4B**).

Table 2. Estimate of the number of functional $K_V7.2$-5 channels expressed from macroscopic current recordings in *Xenopus* oocytes

	$K_V7.2$	$K_V7.3$	$K_V7.4$	$K_V7.5$
P_o	0.17	0.89	0.07	0.17
i (pA) at 0 mV	0.55	0.64	0.21	0.19
Single-channel conductance (g, pS)	6.2	8.5	2.1	2.2
Macroscopic current measured at 0 mV (nA)	548 (n = 8)	95 (n = 4)	286 (n = 3)	402 (n = 6)
Estimated channel number	≈5.800.000	≈166	≈19.500.000	≈12.500.000

P_o, i and g data are from Li et al.[46]

Q_{ON} charge was calculated by integrating the transient outward current elicited at +40 mV; the pooled results obtained in oocytes expressing the different neuronal K_V7 channels are shown in **Figure 4C**. While the amount of charge calculated in $K_V7.2$- and $K_V7.3$-expressing oocytes was not significantly different from those of uninjected oocytes, Q_{ON} values of $K_V7.4$ and $K_V7.5$ channels were 1.34 ± 0.34 and 0.79 ± 0.20 nC, respectively ($p < 0.05$ when compared to uninjected controls).

In addition, although the simultaneous expression of $K_V7.2$ and $K_V7.3$ subunits is known to generate ionic currents which are larger than those recorded upon expression of $K_V7.2$ or $K_V7.3$ subunits alone,[41,42] possibly as a consequence of an increased subunit expression in the membrane,[43] no gating currents could be recorded upon $K_V7.2$ and $K_V7.3$ heteromeric expression (Q_{ON} values were 0.09 ± 0.06 nC, n = 8; $p > 0.05$ vs. controls). Similar

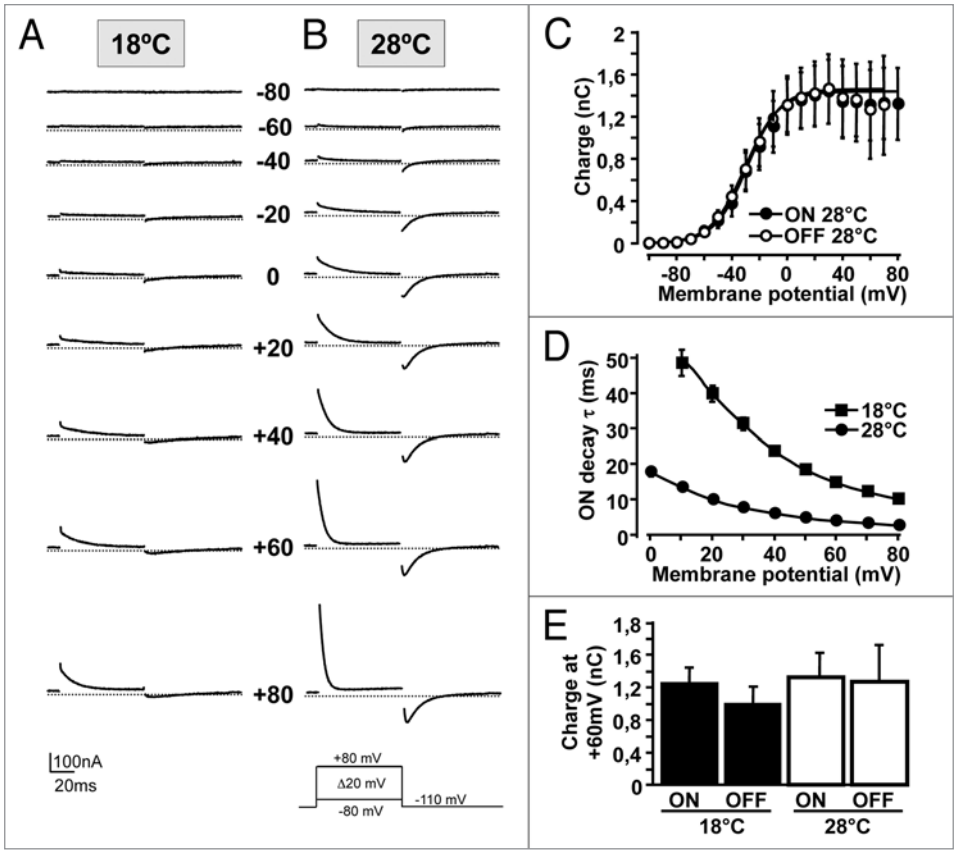

Figure 5. Kinetic and steady state properties of $K_V7.4$ gating currents. Representative gating currents recorded at 18°C (A) and 28°C (B) from $K_V7.4$ channels expressed in *Xenopus* oocytes. The records have been subtracted using the p/-8 protocol; given the high recording bandwidth (50 kHz), a few points of the recordings appear not to be properly subtracted by this procedure. Therefore, we erased the data points corresponding to one ms after the onset of the depolarizing and repolarizing pules. (C) Q_{ON} (filled symbols) and Q_{OFF} (empty symbols) steady-state activation curve; Q_{ON} and Q_{OFF} absolute values were calculated as described. Continuous lines represent Boltzmann fits of the experimental data. (D) Q_{ON} decay time constants obtained at 18°C (filled squares) and 28°C (filled circles) plotted versus membrane potentials. (E) Comparison between Q_{ON} and Q_{OFF} values recorded at saturating voltages (+60 mV) at both 18°C and 28°C, as indicated. For (C–E) each value is the Mean ± SEM of 6 determinations.

(negative) results were also obtained upon expression of the chimeras $K_V7.3$(TD;Q1) and $K_V7.3$(P;Q1),[43] or of the $K_V7.3$ A315T mutant (data not shown),[44] all constructs generating larger ionic currents than wild-type $K_V7.3$.

The ability to resolve gating currents is critically dependent on channel density within the membrane. This is a major potential limitation for K_V7 channels whose plasma membrane/cytosol expression ratio is relatively low.[42,45] The fact that in the present recordings gating current could be only detected in $K_V7.4$- and $K_V7.5$-expressing oocytes, appears to suggest that the density of these channels in the oocyte plasma membrane is higher that of $K_V7.2$ and $K_V7.3$. This view seems to be supported by the data shown in **Table 2**, where the putative number of channels expressed in the membrane is calculated from an independent measurement, namely the ionic current density. The maximal macroscopic current (*I(V)*) is related to the number of channels (*n*) by the following relation

$$I(V) = n\, p_o(V)\, i(V)$$

where $p_o(V)$ is the maximal opening probability, and $i(V)$ is the single-channel current. Using the known values for $p_o(V)$ and $i(V)$ for each neuronal K_V7 channel subtype,[46] we estimated that the membrane expression level of $K_V7.4$ subunits is the highest, with $K_V7.5$ subunits being expressed at about half of the $K_V7.4$ levels. Interestingly, similar calculations indicate that lower expression levels would be expected for $K_V7.2$ and much more so for $K_V7.3$ subunits. Collectively, these data strongly support the hypothesis that the transient outward and inward currents recorded from $K_V7.4$- and $K_V7.5$-expressing oocytes upon complete blockade of their ionic currents represent, respectively, the ON and OFF gating charges for these channels.

Given that $K_V7.4$-expressing oocytes gave rise to the largest gating currents, subsequent experiments were aimed at defining in more detail their kinetic and steady-state properties.

Gating currents from $K_V7.4$ channels. *Effect of temperature.* Representative $K_V7.4$ gating currents recorded in response to variable test potentials at 18°C and 28°C are shown in **Figure 5A and B**, respectively. At 18°C, and in the presence of 2 mM Ba^{2+}_e, small Q_{ON} and Q_{OFF} gating currents appeared around -40 mV (**Fig. 5A**); Q_{ON} and Q_{OFF} values increased at more depolarized potentials (from -40 mV to +80 mV), reaching saturation around +60 mV. While the resolution of Q_{ON} rising kinetics was limited by the speed of the clamp, its subsequent decay was much slower and well resolved around threshold potentials and its time constant decreased at more depolarized membrane potential values (**Fig. 5D**). By contrast, Q_{OFF} activated following a short delay (showing a rising phase), before a much slower deactivation occurred. Q_{OFF} deactivation, whose kinetics was too slow to be analyzed, did not appear to change significantly when more depolarized membrane potentials were applied during the test pulses. Given the slow Q_{ON} and Q_{OFF} decays at 18°C, which substantially impeded an exhaustive analysis of charge movement as a function of voltage at this temperature, Q_{ON}/V and Q_{OFF}/V curves were not evaluated; nevertheless, it appears as, at very depolarized values of membrane potential (+60 mV), the maximal Q_{ON} and Q_{OFF} values were similar, indicating charge conservation (**Fig. 5E**).

Increasing the recording temperature from 18°C to 28°C allowed to detect significant amounts of Q_{ON} when the cells were depolarized at membrane potential values above -60 mV (**Fig. 5B**); at this higher recording temperature, Q_{ON} decay kinetics were faster (**Fig. 5D**), whereas, similarly to 18°C, Q_{ON} rising phase was time independent (almost instantaneous). When repolarized to -110 mV, Q_{OFF} showed a clear rising phase, particularly evident when the potential values during the pulses were more positive than 0 mV. Compared to the 18°C recordings, Q_{OFF} decay appeared to be markedly accelerated.

Figure 5C shows the voltage-dependence of the absolute values of Q_{ON} and Q_{OFF} time integrals recorded at 28°C; fitting the experimental values of the Q_{ON}/V and Q_{OFF}/V curves with a Boltzmann equation, resulted in $V_{½}$ and k values of -26.3 ± 2.3 and 12.6 ± 1.2 for Q_{ON}/V, and -27.6 ± 1.7 and 14 ± 1.1 for Q_{OFF}/V. Also, the fact that the maximal absolute values of ON and OFF charges calculated at depolarized membrane potential values (+60 mV) were similar, clearly indicated the lack of OFF gating charge immobilization. Moreover, at +60 mV, maximal Q_{ON} and Q_{OFF} values at 28°C did not differ from those at 18°C (**Fig. 5E**).

Effect of barium on K_V7.4 ionic current and correlation with gating currents. Gating current measurements herewith reported were performed in the presence of 2 mM Ba^{2+} ions in the extracellular solution. In order to allow a direct comparison between the voltage-dependence of the gating charge movement with that of channel opening for K_V7.4 channels, experiments were performed to assess the effects of Ba^{2+} ions on K_V7.4 channel ionic currents at 28°C. As shown in **Figure 6A**, the presence of 2 mM Ba^{2+} in the extracellular solution caused a significant (>70%) blockade of the ionic currents carried by K_V7.4 channels; moreover, after addition of extracellular Ba^{2+}, an instantaneous, fast-rising transient current component was observed in response to strong depolarizations (see insert to **Fig. 6A**), likely corresponding to the ON gating charge of the expressed channels. Ba^{2+} ions appeared to exert complex effects on K_V7.4 channels, causing a dramatic slowing down of current activation kinetics (the activation τ_s at +40 mV were 191 ± 9.5 ms and 1465 ± 510 ms in the absence and in the presence of 2 mM extracellular Ba^{2+}, respectively; n = 3–6), together with a >50 mV rightward shift in the apparent steady-state voltage-dependence of activation (**Fig. 6B**); these effects appeared qualitatively similar to those previously described for K_V7.1 channels[40] (see discussion). Despite these effects, direct comparison of the steady-state properties of the G/V curve with those of the Q/V curve measured under identical conditions (in the presence of 2 mM Ba^{2+} ions in the extracellular solution) shows that the Q/V curve displayed a $V_{½}$ value at least 50 mV more negative than that of the G/V curve. It is important to note that even when the Q/V curve (obtained with 2 mM Ba^{2+}) was compared to the G/V curve recorded in the absence of Ba^{2+}_e, a significant 10 mV negative shift of the Q/V curve to more hyperpolarized potentials was observed. These results show that there is significant charge movement among closed states.

Finally, **Figure 6C** shows K_V7.4 gating and ionic current kinetics on the same time scale at +40 mV. Ionic currents were recorded in control solution (no external blocker added); gating currents were recorded in TEA-based solutions plus 2 mM Ba^{2+}_e. Even despite such intrinsic limitation, these kinetic data suggest most of the gating charge in K_V7.4 channels is moved among closed states, well before channel opening, in agreement with the steady state data shown in **Figure 6B**.

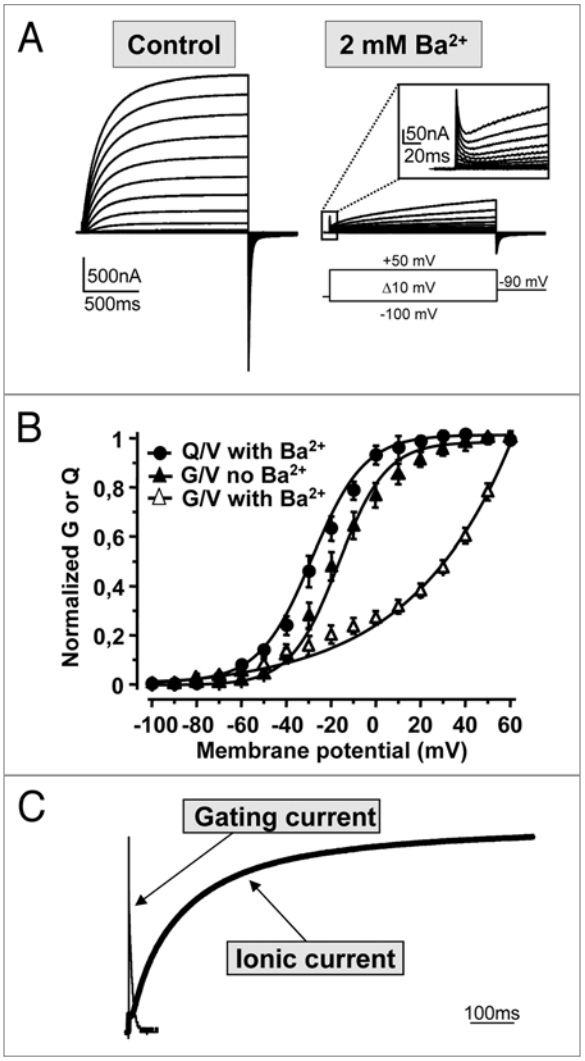

Figure 6. Effect of extracellular Ba^{2+} on the macroscopic currents from K_V7.4 homomeric channels, and correlation between ionic and gating currents. (A) K_V7.4 ionic current were elicited at 28°C in response to test pulses from -100 to +50 mV in 10 mV increments from and returning to an holding potential of -90 mV in the absence or in the presence of 2 mM Ba^{2+} in the external solution, as indicated. The insert shows an enlargement of the initial current responses to depolarizing pulses. (B) Comparison between the G/V curves for K_V7.4 obtained with (empty triangles) or without (filled triangles) 2 mM extracellular Ba^{2+}, and the Q_{ON}/V curve for K_V7.4 (filled circles) recorded in TEA-based solutions containing 2 mM extracellular Ba^{2+}. Continuous lines for the G/V (in the absence of Ba^{2+}) and of the Q_{ON}/V (in the presence of Ba^{2+}) curves represent Boltzmann fits of the experimental data; $V_{½}$ and k values were -16.7 ± 1.4 and 10.7 ± 0.6 (G/V) and -26.3 ± 2.3 and 12.6 ± 1.2 (Q_{ON}/V). Each value is the Mean ± SEM of 4–8 determinations. (C) Comparison of K_V7.4 gating and ionic current kinetics on the same time scale at +40 mV. Ionic currents were recorded in control solution (no external blocker added); gating currents were recorded in TEA-based solutions plus 2 mM extracellular Ba^{2+}.

Discussion

K_V7 channels achieve their specific functional role in cellular excitability control by means of a precise regulation of their gating properties; therefore, investigation of the molecular mechanisms controlling gating appears crucial to our understanding of K_V7 channels pathophysiological role. Since gating currents measurements represent a direct measure of VSD displacement in response to changes in the membrane electric field,[47] the aims of this work have been to record gating currents from homomeric neuronal K_V7 channels expressed in *Xenopus* oocytes using the open-oocyte vaseline-gap technique,[32] to find the appropriate experimental conditions allowing to characterize their kinetic and steady-state properties, and to correlate these properties with those of the ionic currents.

K_V7 channels are characterized by their slow gating; activation and deactivation time constants, when measured at extreme depolarizing or hyperpolarizing potentials, respectively, are in the range of 20–100 ms.[48,49] This fact, together with the low abundance of channels in the plasma membrane relative to the cytoplasm,[42,45] is a major challenge when attempting to measure gating current. In the present work, gating currents were clearly detected in *Xenopus* oocytes expressing $K_V7.4$ and $K_V7.5$ channels, whereas homomeric $K_V7.2$ or $K_V7.3$, as well as heteromeric $K_V7.2/K_V7.3$ channels, failed to give rise to currents attributable to VSD displacement within the membrane electric field. These results, in large agreement with those derived from calculations of the number of functional channels from macroscopic and single channel recordings, indicate that, in *Xenopus* oocytes, the membrane density of functional $K_V7.4$ and $K_V7.5$ channels is considerably higher than that of $K_V7.2$ and $K_V7.3$; also in mammalian cells, functional $K_V7.4$ channel density appears 30–300 times higher than that of $K_V7.2$ or $K_V7.3$ channels.[50] However, caution should be exercised when calculating channel densities from current measurements, since the results from biochemical and optical techniques in both *Xenopus* oocytes and mammalian cells have revealed that, despite large differences in current sizes, the plasma membrane density of channel subunits appears rather similar among different K_V7 members.[44,50] These results suggest that most K_V7 channels may be present in the plasma membrane in a functionally silent (non conductive) state;[50] for $K_V7.3$, specific structural constraints within the pore act as crucial regulators of the ratio among conductive and non-conductive channels at the plasma membrane, since mutations affecting the conduction pathway (such as the replacement of the alanine at position 315 with a threonine) can dramatically influence such parameter, leading to a large increase in current size. Nevertheless, in our experiments, we were unable to detect gating currents not only from wild-type $K_V7.3$, but also from $K_V7.3$ A315T mutant channels, suggesting that mechanisms additional to pore conformation, possibly related to homomers/heteromers formation or glycosylation,[43] retention/retrieval signals,[51] or interaction with intracellular regulators such as calmodulin,[52] phosphatidylinositol 4,5-bisphosphate,[53] or ankyrin-G,[54] might contribute to the differential plasma membrane density of functional neuronal K_V7 subunits.

Transient outward and inward currents recorded upon depolarization and subsequent repolarization, respectively, from $K_V7.4$-expressing oocytes after ionic current blockade with TEA and Ba^{2+} can be regarded as gating currents because they were never observed in uninjected oocytes or, as previously mentioned, in $K_V7.2$- and $K_V7.3$-expressing oocytes, their time integral well correlated with the size of the ionic current, and they had some typical properties of gating currents. These include: (1) an increased size of the time integrals of both outward and inward currents with more depolarized potentials, reaching saturation around 0 mV; (2) a faster decay of the transient outward current with increasing voltages; (3) a rising phase in the inward current evoked upon repolarization to negative potentials after depolarizations to values >0 mV. These characteristics allowed to conclude that the transient outward and inward currents recorded from $K_V7.4$-expressing oocytes represent the Q_{ON} and the Q_{OFF} gating currents from $K_V7.4$ channels, respectively.

In these experiments, $K_V7.4$ Q_{ON} and Q_{OFF} were recorded at 28°C, since temperature is known to speed-up channel gating, thus improving the resolution of slow kinetic processes;[47] in fact, Q_{ON} and the Q_{OFF} were also recorded at 18°C, although they displayed markedly slower kinetics. The estimated Q_{10} for $K_V7.4$ activation was 8.3, the highest among neuronal K_V7 channels and similar to that of Shaker B channels (>4)[34] and of KCNE1/$K_V7.1$ channels (≈7.3);[55] in agreement with these studies, no significant changes in the voltage-dependence of channel activation were observed between 18°C and 28°C. Because of the high Q_{10} value, $K_V7.4$ macroscopic currents required several seconds to reach steady-state conditions at 18°C; moreover, at lower temperatures, gating current kinetics (Q_{OFF} in particular) were poorly resolved.

For some preparations, including the gating currents from squid axon Na^+ channels,[56] and those from K^+ channels from Drosophila and rat brain expressed in oocytes,[24,57] the Q_{OFF} failed to quickly recover at the end of a depolarizing pulse, a phenomenon known as charge immobilization. Charge immobilization has been mostly linked to channel entry in an inactivated state, either from the open,[24] or from the closed state (such as in skeletal muscle Na^+ channels);[58] on the other hand, charge immobilization is absent in the gating currents recorded from channels carrying non-inactivating currents, such as $K_V2.1$,[25] inactivation removed Shaker B,[59] and EAG channels.[29] In the present experiments, the maximal absolute values of the Q_{ON} and Q_{OFF} gating currents from oocytes expressing $K_V7.4$ channels were identical, suggesting that charge immobilization did not occur. This may correlate with the absence of macroscopic current inactivation within the short (70 ms) durations of our depolarizing pulses; in fact, much longer (>20 sec) pulses were needed to promote inactivation in $K_V7.4$ and $K_V7.5$ channels.[60]

As anticipated, one characteristic feature of the macroscopic currents carried by $K_V7.4$ channels is their slow activation kinetics; the observed fast decay of Q_{ON} with respect to the slow ionic current activation kinetics suggests that there are rate limiting steps following the fast charge movement mostly occurring in transitions among closed states. Thus, closed states in the vicinity of the open state carry small amount of charge or they are too slow to be detected. This result appears consistent with the

idea that slow VSD movement during channel activation do not account for the slow kinetics of $K_V7.4$ currents, which are mainly due to the presence of slower and less voltage-dependent transitions closer to the open state; this view seems strongly supported by the observation that, particularly after stronger depolarizations leading to channel opening, Q_{OFF} return was delayed.

The hypothesis that, in $K_V7.4$ channels a large fraction of the voltage-dependence occurs in transitions between closed states seems also consistent with the more negative position of the Q_{ON}/V curve versus the G/V curve along the voltage axis. However, it should be noticed that, in order to achieve a significant blockade of the $K_V7.4$ macroscopic currents, 2 mM Ba^{2+} was added to the TEA-based extracellular recording solution. Ba^{2+} ions, in contrast to TEA, which behaves in most instance as a pure open-channel blocker,[41] are known to exert complex effects on VGKCs,[61-63] often leading to dramatic changes of several components of the gating process. Although Ba^{2+} block has not been studied in detail in neuronal K_V7 channels, Gibor et al.[40] recently reported that external Ba^{2+} interacts with cardiac $K_V7.1$ channels with two sites, both located in the conduction pathway: one deep in the pore and responsible for a voltage-dependent block of the conduction, and another more superficial affecting channel gating with only minor effect on K^+ conduction. Similarly, in rod photoreceptors of tiger salamanders, the conductance of I_{Kx}, a voltage-dependent K^+ current that shows many similarities to I_{KM}, was reduced and shifted toward more positive potentials by external Ba^{2+}.[64] Qualitatively similar results were observed in our experiments, since the addition of 2 mM extracellular Ba^{2+} caused a voltage-dependent block of $K_V7.4$ macroscopic currents, and led to an apparent positive shift of their voltage-dependence of at least 50 mV. As we do not know whether and by what extent Ba^{2+} might be affecting the voltage dependence of the gating current as compared to the ionic current, we cannot establish at present an exact relationship between gating and conduction. However, even if we consider the extreme case that Ba^{2+} would not affect the kinetic and steady-state properties of the gating currents, comparison of the ionic currents without Ba^{2+} and the gating currents in the presence of Ba^{2+} shows that there is charge movement at potentials where the channels are not conducting, a clear indication that a significant amount of charge is moved among closed states. The existence of distinct channel conformations corresponding to different closed states has been recently proposed for $K_V7.1$ channels on the basis of homology modeling results.[65]

In conclusion, the present results describe for the first time the gating currents from $K_V7.4$ and $K_V7.5$ channels expressed in *Xenopus* oocytes. Mutations in four of the five members of the K_V7 channel family are responsible for human channelopathies, with phenotypical consequences ranging from neonatal epilepsy ($K_V7.2$ and $K_V7.3$), to cardiac arrhythmias ($K_V7.1$), to deafness ($K_V7.4$).[17] A large number of these mutations affect residues located within the VSD and alter the gating properties of the channel macroscopic currents; therefore, in future experiments, it will be of interest to investigate the functional consequences on gating current behavior of disease-causing mutations which modify macroscopic current gating properties.[14-16,18] A feature of $K_V7.4$ gating currents seems to be a clear separation along the voltage axis between the Q_{ON}/V and the G/V curves, suggestive of a very slow or low bearing charge step that couples the VSD displacement and channel opening. Therefore, the occupancy of intermediate channel configurations toward channel opening through voltage-independent transitions may also provide a theoretical framework to interpret the molecular consequence of disease-causing mutations affecting channel gating and located in the S_4-S_5 linker region or the S_6 inner pore gate, channel regions located outside of the VSD but involved in the electromechanical coupling between VSD movement and pore opening.[66,67] Noticeably, these regions are involved in binding of neuronal K_V7 channels modulators,[43,68] which appear as promising therapeutic tools against hyperexcitability diseases.[2]

Materials and Methods

Isolation of *Xenopus* oocytes. The dissociation, maintenance and microinjection of *Xenopus* oocytes followed standard procedures.[31] Briefly, ovarian lobes were surgically removed from adult female *Xenopus* frogs and individual oocytes dissociated by enzymatic treatment with collagenase (type II; 1 mg/ml) for 60 min in a Ca^{2+}-free solution. Once dissociated, Ca^{2+} was reintroduced in the oocyte-bathing solution and the oocytes were stored at 18°C for use on the following day.

cDNA transcription and oocyte injection. $K_V7.2$, $K_V7.3$ and $K_V7.4$ cDNAs were cloned in pTLN vectors, whereas $K_V7.5$ was in pSRC5. These plasmids were linearized using MluI ($K_V7.2$ and $K_V7.4$), HpaI ($K_V7.3$) or ApaLI ($K_V7.5$) restriction enzymes, and transcribed in vitro with a commercially available kit (Ambion, Austin, TX) using SP6 ($K_V7.2$, $K_V7.3$ or $K_V7.4$) or T7 ($K_V7.5$) RNA polymerases. RNAs were quantified spectrophotometrically and stored at -80°C. *Xenopus* oocytes were microinjected with 50 nl of 1 μg/μl RNA. After injection, the oocytes were incubated at 18°C in a solution containing 10 mM NaCl, 83 mM KCl, 1 mM $MgCl_2$, 1.8 mM $CaCl_2$ and 5 mM Hepes, pH 7.5 with NaOH, supplemented with gentamycin.

Electrophysiology. Ionic and gating currents from *Xenopus* oocytes were measured 3–4 days after RNA injection, using the vaseline-gap cut-open voltage-clamp (COVC) technique.[32,33] The temperature was controlled by a Peltier device with negative feedback using a thermistor as a temperature sensor.

For ionic current recordings, the external and internal solutions contained (in mM): 101 N-Methy-D-Glucamine (NMG), 12 KOH, 4 $Ca(OH)_2$ and 20 Hepes, pH 7.4 with methane sulfonic acid (MES acid), and 120 KOH, 2 EGTA and 20 Hepes, pH 7.4 with MES acid, respectively. For gating current recordings, the external and internal solutions contained (in mM): 100 tetraethylammonium-hydroxide (TEA-OH), 2 $Ca(OH)_2$, 2 $BaCl_2$ and 20 Hepes, pH 7.4 with MES acid, and 115 TEA-OH, 2 EGTA and 20 Hepes, pH 7.4 with MES acid, respectively. Oocytes were permeabilized by adding 0.3% saponin to the lower chamber for ~1 min. Microelectrodes were pulled from borosilicate glass capillary tubes to obtain a resistance of 0.1–0.5 MΩ when filled with 3 M CsMES +20 mM CsCl.

Ionic currents from expressed channels were activated by holding the oocytes at -90 mV (holding potential = -90) and

then applying pulses of 1.5 s durations from -100 to +40 mV, in increments of 10 mV, returning to the holding potential. Capacity currents were compensated by analog circuitry and subtracted on-line by using a p/-8 protocol from a holding potential of -80 mV; in some cases, the subtraction was done off-line. Data were filtered at 1–2 kHz and sampled at 2–4 kHz. For gating current recordings, oocytes were maintained at 0 mV for 30 min to deplete intracellular K^+; after this period, the cells were exposed to the TEA- and Ba^{2+}-based solutions, and the following protocol was applied: from a holding potential of -90 mV, a short (20 ms) pulse to -110 mV was followed by a series of progressively increasing depolarizations (from -80 mV to +80 mV) of 70 ms duration, before a final 70 ms step to -110 mV was applied. Data were filtered at 5 kHz and sampled at 50 kHz. Capacitance currents were compensated by analog circuitry and subtracted on-line by using a p/-8 protocol from a subtracting holding potential of -100 mV.

Data analysis and statistics. In ionic current recordings, extracellular K^+ accumulation during the depolarizing pulse caused a progressive rise in inward current size upon hyperpolarization, thereby impeding tail current analysis, conductance (G) values were calculated as follows: given V_1 the voltage in the depolarizing pulse and V_2 the return potential voltage, the current were measured at the end of the V_1 pulse (I_1) and at the V_2 tail peak (I_2). Then:

$$I_1 = G(V_1 - V_e), \text{ and } I_2 = G(V_2 - V_e)$$

where V_e is the K^+ equilibrium potential; G is the same because it has no time to change from the end to the pulse to the beginning of the tail. From these equations, G can be calculated according to the following equation:

$$I_1 - I_2 = G(V_1 - V_2)$$

The G values obtained by this method are thus independent on the K^+ equilibrium potential (therefore not influenced by changes in V_e caused by K^+ accumulation) and are only minimally influenced by fast and voltage-dependent outward current blockade by intracellular cations. Conductance values were expressed as a function of membrane potential, and the data were then fit to a Boltzmann distribution of the following form:

$$y = max/[1 + exp(V_{1/2} - V)/k]$$

where V is the test potential, $V_{1/2}$ is the half-activation potential, and k is the slope factor. Activation kinetics were analyzed by fitting the current traces elicited by depolarization with a single-($y = A\ exp(-t/\tau) + c$) or a double-exponential equation

$$y = A_f\, exp(-t/\tau_f) + A_s\, exp(-t/\tau_s) + c$$

where A_f and A_s indicate the amplitude of the *fast* and *slow* exponential components, τ_f and τ_s the time constants of each component, and c is an offset value. For the traces fit with a double exponential, τ was calculated with the following equation:

$$\tau = (\tau_f A_f + \tau_s A_s)/(A_f + A_s)$$

thus obtaining a single time constant representing the weighed average of the slow and fast components.

In gating current recordings, gating charge (Q) was calculated as the time integral of the sensing currents at each potential after leak subtraction. Q was plotted as a function of membrane potential, and the data were then fit to the previously described form of the Boltzmann equation. For both macroscopic and gating current recordings, data acquisition and analysis were carried out with in-house developed software. Data are expressed as Means ± SEM of the given number of experiments (n). Data sets were compared using matched Student's t tests or, if necessary, with one-way ANOVA, followed by the Newman Keul's test. Statistically significant differences were accepted when p was <0.05.

Acknowledgements

We are deeply indebted to Prof. Thomas J. Jentsch (Department of Physiology and Pathology of Ion Transport, Leibniz-Institut für Molekulare Pharmakologie, Berlin-Buch, Germany), Alvaro Villarroel (Unidad de Biofísica, CSIC-UPV/EHU, Universidad del País Vasco, Leioa, Spain), Mark Shapiro (Department of Physiology, UTHSCniversity of Texas Health Science Center at San Antonio, San Antonio, Texas, USA), and Michael Schwake (Institute of Biochemistry, Christian-Albrechts-University Kiel, Kiel, Germany) for sharing plasmids. The Authors appreciate the help from Fabiana Vasconcelo Campos and Walter Sandtner for initial help with electrophysiology and molecular biology experiments, respectively, at the University of Chicago. The present study was supported by grants from: Telethon GP07125 and PRIN 2007 to Maurizio Taglialatela, E-Rare JTC 2007 to Maria Roberta Cilio, and by NIH grant GM30376 to Francisco Bezanilla.

References

1. Miller C. An overview of the potassium channel family. Genome Biol 2000; 1:4.
2. Miceli F, Soldovieri MV, Martire M, Taglialatela M. Molecular pharmacology and therapeutic potential of neuronal K_V7-modulating drugs. Curr Opin Pharmacol 2008; 8:65-74.
3. Schroeder BC, Hechenberger M, Weinreich F, Kubisch C, Jentsch TJ. KCNQ5, a novel potassium channel broadly expressed in brain, mediates M-type currents. J Biol Chem 2000; 275:24089-95.
4. Roura-Ferrer M, Sole L, Martinez-Marmol R, Villalonga N, Felipe A. Skeletal muscle K_V7 (KCNQ) channels in myoblast differentiation and proliferation. Biochem Biophys Res Commun 2008; 369:1094-7.
5. Yeung SY, Pucovsky V, Moffatt JD, Saldanha L, Schwake M, Ohya S, Greenwood IA. Molecular expression and pharmacological identification of a role for K(v)7 channels in murine vascular reactivity. Br J Pharmacol 2007; 151:758-70.
6. Sanguinetti MC, Jurkiewicz NK. Two components of cardiac delayed rectifier K^+ current. Differential sensitivity to block by class III antiarrhythmic agents. J Gen Physiol 1990; 96:195-215.
7. Sanguinetti MC, Curran ME, Zou A, Shen J, Spector PS, Atkinson DL, Keating MT. Coassembly of K(V) LQT1 and minK (IsK) proteins to form cardiac I(Ks) potassium channel. Nature 1996; 384:80-3.
8. Wang Q, Curran ME, Splawski I, Burn TC, Millholland JM, VanRaay TJ, et al. Positional cloning of a novel potassium channel gene: KVLQT1 mutations cause cardiac arrhythmias. Nat Genet 1996; 12:17-23.
9. Brown DA, Adams PR. Muscarinic suppression of a novel voltage-sensitive K^+ current in a vertebrate neurone. Nature 1980; 283:673-6.
10. Kubisch C, Schroeder BC, Friedrich T, Lutjohann B, El-Amraoui A, Marlin S, et al. KCNQ4, a novel potassium channel expressed in sensory outer hair cells, is mutated in dominant deafness. Cell 1999; 96:437-46.
11. Biervert C, Schroeder BC, Kubisch C, Berkovic SF, Propping P, Jentsch TJ, Steinlein OK. A potassium channel mutation in neonatal human epilepsy. Science 1998; 279:403-6.

12. Charlier C, Singh NA, Ryan SG, Lewis TB, Reus BE, Leach RJ, Leppert M. A pore mutation in a novel KQT-like potassium channel gene in an idiopathic epilepsy family. Nat Genet 1998; 18:53-5.
13. Singh NA, Charlier C, Stauffer D, DuPont BR, Leach RJ, Melis R, et al. A novel potassium channel gene, KCNQ2, is mutated in an inherited epilepsy of newborns. Nat Genet 1998; 18:25-9.
14. Dedek K, Kunath B, Kananura C, Reuner U, Jentsch TJ, Steinlein OK. Myokymia and neonatal epilepsy caused by a mutation in the voltage sensor of the KCNQ2 K^+ channel. Proc Natl Acad Sci USA 2001; 98:12272-7.
15. Castaldo P, del Giudice EM, Coppola G, Pascotto A, Annunziato L, Taglialatela M. Benign familial neonatal convulsions caused by altered gating of KCNQ2/KCNQ3 potassium channels. J Neurosci 2002; 22:RC199.
16. Panaghie G, Abbott GW. The role of S_4 charges in voltage-dependent and voltage-independent KCNQ1 potassium channel complexes. J Gen Physiol 2007; 129:121-33.
17. Soldovieri MV, Miceli F, Bellini G, Coppola G, Pascotto A, Taglialatela M. Correlating the clinical and genetic features of benign familial neonatal seizures (BFNS) with the functional consequences of underlying mutations. Channels (Austin) 2007; 1:228-33.
18. Miceli F, Soldovieri MV, Hernandez CC, Shapiro MS, Annunziato L, Taglialatela M. Gating consequences of charge neutralization of arginine residues in the S_4 segment of K(v)7.2, an epilepsy-linked K^+ channel subunit. Biophys J 2008; 95:2254-64.
19. Armstrong CM, Bezanilla F. Currents related to movement of the gating particles of the sodium channels. Nature 1973; 242:459-61.
20. Aggarwal SK, MacKinnon R. Contribution of the S_4 segment to gating charge in the Shaker K^+ channel. Neuron 1996; 16:1169-77.
21. Seoh SA, Sigg D, Papazian DM, Bezanilla F. Voltage-sensing residues in the S_2 and S_4 segments of the Shaker K^+ channel. Neuron 1996; 16:1159-67.
22. Bezanilla F. How membrane proteins sense voltage. Nat Rev Mol Cell Biol 2008; 9:323-32.
23. Tombola F, Pathak MM, Isacoff EY. How does voltage open an ion channel? Annu Rev Cell Dev Biol 2006; 22:23-52.
24. Bezanilla F, Perozo E, Papazian DM, Stefani E. Molecular basis of gating charge immobilization in Shaker potassium channels. Science 1991; 254:679-83.
25. Taglialatela M, Stefani E. Gating currents of the cloned delayed-rectifier K^+ channel DRK1. Proc Natl Acad Sci USA 1993; 90:4758-62.
26. Fedida D, Bouchard R, Chen FS. Slow gating charge immobilization in the human potassium channel $K_V1.5$ and its prevention by 4-aminopyridine. J Physiol 1996; 494:377-87.
27. Stefani E, Ottolia M, Noceti F, Olcese R, Wallner M, Latorre R, Toro L. Voltage-controlled gating in a large conductance Ca^{2+}-sensitive K^+ channel (hslo). Proc Natl Acad Sci USA 1997; 94:5427-31.
28. Dougherty K, Covarrubias M. A dipeptidyl aminopeptidase-like protein remodels gating charge dynamics in $K_V4.2$ channels. J Gen Physiol 2006; 128:745-53.
29. Tang CY, Bezanilla F, Papazian DM. Extracellular Mg(2+) modulates slow gating transitions and the opening of Drosophila ether-a-Go-Go potassium channels. J Gen Physiol 2000; 115:319-38.
30. Piper DR, Varghese A, Sanguinetti MC, Tristani-Firouzi M. Gating currents associated with intramembrane charge displacement in HERG potassium channels. Proc Natl Acad Sci USA 2003; 100:10534-9.
31. Goldin AL, Sumikawa K. Preparation of RNA for injection into *Xenopus* oocytes. Methods Enzymol 1992; 207:279-97.
32. Taglialatela M, Toro L, Stefani E. Novel voltage clamp to record small, fast currents from ion channels expressed in *Xenopus* oocytes. Biophys J 1992; 61:78-82.
33. Stefani E, Bezanilla F. Cut-open oocyte voltage-clamp technique. Methods Enzymol 1998; 293:300-18.
34. Rodriguez BM, Sigg D, Bezanilla F. Voltage gating of Shaker K^+ channels. The effect of temperature on ionic and gating currents. J Gen Physiol 1998; 112:223-42.
35. Benham CD, Gunthorpe MJ, Davis JB. TRPV channels as temperature sensors. Cell Calcium 2003; 33:479-87.
36. Perozo E, MacKinnon R, Bezanilla F, Stefani E. Gating currents from a nonconducting mutant reveal open-closed conformations in Shaker K^+ channels. Neuron 1993; 11:353-8.
37. Hadley JK, Noda M, Selyanko AA, Wood IC, Abogadie FC, Brown DA. Differential tetraethylammonium sensitivity of KCNQ1-4 potassium channels. Br J Pharmacol 2000; 129:413-5.
38. Kotani S, Hirasawa T, Suzuki T, Sato K, Sakakibara M, Tokimasa T. Mechanisms underlying the M-current block by barium in bullfrog sympathetic neurons. Neurosci Lett 2000; 285:1-4.
39. Robbins J. KCNQ potassium channels: physiology, pathophysiology and pharmacology. Pharmacol Ther 2001; 90:1-19.
40. Gibor G, Yakubovich D, Peretz A, Attali B. External barium affects the gating of KCNQ1 potassium channels and produces a pore block via two discrete sites. J Gen Physiol 2004; 124:83-102.
41. Wang HS, Pan Z, Shi W, Brown BS, Wymore RS, Cohen IS, et al. KCNQ2 and KCNQ3 potassium channel subunits: molecular correlates of the M-channel. Science 1998; 282:1890-3.
42. Soldovieri MV, Castaldo P, Iodice L, Miceli F, Barrese V, Bellini G, et al. Decreased subunit stability as a novel mechanism for potassium current impairment by a KCNQ2 C terminus mutation causing benign familial neonatal convulsions. J Biol Chem 2006; 281:418-28.
43. Schenzer A, Friedrich T, Pusch M, Saftig P, Jentsch TJ, Grotzinger J, Schwake M. Molecular determinants of KCNQ (K_V7) K^+ channel sensitivity to the anticonvulsant retigabine. J Neurosci 2005; 25:5051-60.
44. Etxeberria A, Santana-Castro I, Regalado MP, Aivar P, Villarroel A. Three mechanisms underlie KCNQ2/3 heteromeric potassium M-channel potentiation. J Neurosci 2004; 24:9146-52.
45. Shah MM, Mistry M, Marsh SJ, Brown DA, Delmas P. Molecular correlates of the M-current in cultured rat hippocampal neurons. J Physiol 2002; 544:29-37.
46. Li Y, Gamper N, Shapiro MS. Single-channel analysis of KCNQ K^+ channels reveals the mechanism of augmentation by a cysteine-modifying reagent. J Neurosci 2004; 24:5079-90.
47. Bezanilla F. The voltage sensor in voltage-dependent ion channels. Physiol Rev 2000; 80:555-92.
48. Adams PR, Brown DA, Constanti A. M-currents and other potassium currents in bullfrog sympathetic neurones. J Physiol 1982; 330:537-72.
49. Safiulina VF, Zacchi P, Taglialatela M, Yaari Y, Cherubini E. Low expression of K_V7/M channels facilitates intrinsic and network bursting in the developing rat hippocampus. J Physiol 2008; 586:5437-53.
50. Zaika O, Hernandez CC, Bal M, Tolstykh GP, Shapiro MS. Determinants within the turret and pore-loop domains of KCNQ3 K^+ channels governing functional activity. Biophys J 2008; 95:5121-37.
51. Ekberg J, Schuetz F, Boase NA, Conroy SJ, Manning J, Kumar S, et al. Regulation of the voltage-gated K(+) channels KCNQ2/3 and KCNQ3/5 by ubiquitination. Novel role for Nedd4-2. J Biol Chem 2007; 282:12135-42.
52. Etxeberria A, Aivar P, Rodriguez-Alfaro JA, Alaimo A, Villace P, Gomez-Posada JC, et al. Calmodulin regulates the trafficking of KCNQ2 potassium channels. FASEB J 2008; 22:1135-43.
53. Weixel KM, Edinger RS, Kester L, Guerriero CJ, Wang H, Fang L, et al. Phosphatidylinositol 4-phosphate 5-kinase reduces cell surface expression of the epithelial sodium channel (ENaC) in cultured collecting duct cells. J Biol Chem 2007; 282:36534-42.
54. Pan Z, Kao T, Horvath Z, Lemos J, Sul JY, Cranstoun SD, et al. A common ankyrin-G-based mechanism retains KCNQ and Na_V channels at electrically active domains of the axon. J Neurosci 2006; 26:2599-613.
55. Busch AE, Lang F. Effects of $[Ca^{2+}]_i$ and temperature on minK channels expressed in *Xenopus* oocytes. FEBS Lett 1993; 334:221-4.
56. Bezanilla F, Armstrong CM. Kinetic properties and inactivation of the gating currents of sodium channels in squid axon. Philos Trans R Soc Lond B Biol Sci 1975; 270:449-58.
57. Stuhmer W, Conti F, Stocker M, Pongs O, Heinemann SH. Gating currents of inactivating and non-inactivating potassium channels expressed in *Xenopus* oocytes. Pflugers Arch 1991; 418:423-9.
58. Groome JR, Larsen MF, Coonts A. Differential effects of paramyotonia congenita mutations F1473S and F1705I on sodium channel gating. Channels (Austin) 2008; 2:39-50.
59. Perozo E, Papazian DM, Stefani E, Bezanilla F. Gating currents in Shaker K^+ channels. Implications for activation and inactivation models. Biophys J 1992; 62:160-8.
60. Jensen HS, Grunnet M, Olesen SP. Inactivation as a new regulatory mechanism for neuronal K_V7 channels. Biophys J 2007; 92:2747-56.
61. Armstrong CM, Taylor SR. Interaction of barium ions with potassium channels in squid giant axons. Biophys J 1980; 30:473-88.
62. Taglialatela M, Drewe JA, Brown AM. Barium blockade of a clonal potassium channel and its regulation by a critical pore residue. Mol Pharmacol 1993; 44:180-90.
63. Alagem N, Dvir M, Reuveny E. Mechanism of Ba(2+) block of a mouse inwardly rectifying K^+ channel: differential contribution by two discrete residues. J Physiol 2001; 534:381-93.
64. Wollmuth LP. Mechanism of Ba^{2+} block of M-like K channels of rod photoreceptors of tiger salamanders. J Gen Physiol 1994; 103:45-66.
65. Silva JR, Pan H, Wu D, Nekouzadeh A, Decker KF, Cui J, et al. A multiscale model linking ion-channel molecular dynamics and electrostatics to the cardiac action potential. Proc Natl Acad Sci USA 2009; 106:11102-6.
66. Long SB, Campbell EB, Mackinnon R. Voltage sensor of $K_V1.2$: structural basis of electromechanical coupling. Science 2005; 309:903-8.
67. Long SB, Tao X, Campbell EB, MacKinnon R. Atomic structure of a voltage-dependent K^+ channel in a lipid membrane-like environment. Nature 2007; 450:376-82.
68. Wuttke TV, Seebohm G, Bail S, Maljevic S, Lerche H. The new anticonvulsant retigabine favors voltage-dependent opening of the $K_V7.2$ (KCNQ2) channel by binding to its activation gate. Mol Pharmacol 2005; 67:1009-17.